© 2017. Published by The Company of Biologists Ltd | Development (2017) 144, 3156-3167 doi:10.1242/dev.147256

RESEARCH ARTICLE

Hes5 regulates the transition timing of neurogenesis and gliogenesis in mammalian neocortical development

Shama Bansod[1,2], Ryoichiro Kageyama[1,2,3,4] and Toshiyuki Ohtsuka[1,2,3,*]

ABSTRACT

During mammalian neocortical development, neural stem/progenitor cells (NSCs) sequentially give rise to deep layer neurons and superficial layer neurons through mid- to late-embryonic stages, shifting to gliogenic phase at perinatal stages. Previously, we found that the Hes genes inhibit neuronal differentiation and maintain NSCs. Here, we generated transgenic mice that overexpress Hes5 in NSCs of the central nervous system, and found that the transition timing from deep to superficial layer neurogenesis was shifted earlier, while gliogenesis precociously occurred in the developing neocortex of Hes5-overexpressing mice. By contrast, the transition from deep to superficial layer neurogenesis and the onset of gliogenesis were delayed in *Hes5* knockout (KO) mice. We found that the Hmga genes (*Hmga1*/*2*) were downregulated in the neocortical regions of Hes5-overexpressing brain, whereas they were upregulated in the *Hes5* KO brain. Furthermore, we found that Hes5 expression led to suppression of *Hmga1*/*2* promoter activity. These results suggest that Hes5 regulates the transition timing between phases for specification of neocortical neurons and between neurogenesis and gliogenesis, accompanied by alteration in the expression levels of Hgma genes, in mammalian neocortical development.

KEY WORDS: Hes5, Hmga, Neurogenesis, Gliogenesis, Neocortical development, Mouse

INTRODUCTION

Neural stem/progenitor cells (NSCs) sequentially give rise to deep layer neurons and later to superficial layer neurons; at late embryonic stages, NSCs terminate neurogenesis and shift to gliogenesis. As such, NSCs temporally alter their characteristics, and the timing of the generation of a variety of neurons and glial cells is strictly regulated (McConnell, 1989; Temple, 2001; Ohtsuka et al., 2011). Growing evidence implicates the involvement of epigenetic regulatory systems in the regulation of this transition timing. The polycomb group (PcG) complex of transcriptional repressors has been found to govern the developmental timing of neurogenesis and gliogenesis by modulating histones and chromatin structure during corticogenesis (Vogel et al., 2006; Hirabayashi et al., 2009; Schwartz and Pirrotta, 2013; Pereira et al., 2010; Morimoto-Suzki et al., 2014; Corley and Kroll, 2015). Moreover, it has been reported that the high mobility group AT-hook (Hgma) genes regulate gene expression by modulating chromatin structure (Ozturk et al., 2014), maintain neurogenic NSCs, and inhibit gliogenesis during early- to mid-embryonic stages through global opening of the chromatin state (Kishi et al., 2012). However, the mechanism by which the expression of these epigenetic factors is controlled remains to be analyzed.

Here, we found that Hes5, a transcriptional repressor acting as an effector of Notch signaling, regulates the timing of neurogenesis and gliogenesis via alteration in the expression levels of epigenetic factors. Notch signaling contributes to the elaboration of cellular diversity during the development of various tissues (Kopan et al., 1994; Robey et al., 1996; Weinmaster, 1997; Gridley, 1997; Artavanis-Tsakonas et al., 1999). In addition, in the central nervous system (CNS), Notch signaling governs various developmental processes, such as maintenance of NSCs, neurite outgrowth of cortical neurons, and neuronal versus glial fate choice (de la Pompa et al., 1997; Berezovska et al., 1999; Tanigaki et al., 2001). We previously found that some members of the Hes gene family of basic helix-loop-helix (bHLH) transcriptional repressors (*Hes1/3/5*) function downstream of Notch signaling and inhibit neuronal differentiation (Ishibashi et al., 1994; Ohtsuka et al., 1999, 2001; Kageyama and Ohtsuka, 1999; Hatakeyama et al., 2004). NSCs initially expand as neuroepithelial cells by symmetric proliferative divisions and then transform to radial glial cells (RGCs), a neurogenic form of NSCs, after switching to asymmetric neurogenic divisions. After this transition, differentiating neurons express Notch ligands such as Delta-like (Dll) and Jagged (Jag), and trigger a boost of Notch-Hes signaling in NSCs. Expression of Hes5 is upregulated in RGCs after the onset of neurogenesis, when NSCs start to receive strong intercellular Delta-Notch signals from differentiating and mature neurons (Hatakeyama et al., 2004). Thus, Hes5 is a key regulator of the maintenance of NSCs after the transition to the asymmetric neurogenic division mode.

To more precisely uncover the diverse role of Hes5 throughout the course of neocortical development, we generated transgenic (Tg) mouse lines in which Hes5 expression in NSCs could be manipulated by the Tet-On system. In the Hes5-overexpressing Tg mice, neuronal differentiation from NSCs was strongly inhibited, while the switching from deep to superficial layer neurogenesis was shifted earlier, and gliogenesis was also accelerated and enhanced. By contrast, the transition of neurogenesis and gliogenesis was delayed in the *Hes5* knockout (KO) mice. We found that expression of *Hmga1/2* was suppressed in the neocortical regions of Tg brain; conversely, their expression was upregulated in the *Hes5* KO brain. Furthermore, we found that Hes5 expression led to suppression of the promoter activity of *Hmga1/2* in reporter assays. These results suggest that Hes5 regulates the switching of both neurogenesis and gliogenesis, accompanied by alteration in the expression levels of Hgma genes.

[1]Institute for Frontier Life and Medical Sciences, Kyoto University, 53 Kawahara-cho, Shogoin, Sakyo-ku, Kyoto 606-8507, Japan. [2]Graduate School of Medicine, Kyoto University, Kyoto 606-8501, Japan. [3]Graduate School of Biostudies, Kyoto University, Kyoto 606-8501, Japan. [4]World Premier International Research Initiative-Institute for Integrated Cell-Material Sciences (WPI-iCeMS), Kyoto University, Kyoto 606-8501, Japan.

*Author for correspondence (tohtsuka@infront.kyoto-u.ac.jp)

T.O., 0000-0001-6045-1012

Received 29 November 2016; Accepted 24 July 2017

Development (2017) 144, 3156-3167 doi:10.1242/dev.147256

RESULTS

Overexpression of Hes5 maintained NSCs by inhibiting neuronal differentiation

To manipulate Hes5 expression in NSCs, two Tg mouse lines were generated (Fig. 1A). rtTA was driven in NSCs by the promoter and second intron of the nestin (*Nes*) gene (*pNes-rtTA* Tg). In the presence of doxycycline (Dox), rtTA binds to the Tet-responsive element (TRE) and bidirectionally activates expression of *Hes5* and *d2EGFP* (*TRE-Hes5/d2EGFP* Tg). By crossing both lines, Hes5-overexpressing Tg mice were generated, and Dox (2.0 mg/ml in drinking water) was continuously administered to pregnant mice from embryonic day (E) 9.5 until sacrifice. The whole-body and brain sizes were smaller in the Tg mice than in the wild-type (WT) mice, and GFP was highly expressed in the central nervous system, including the brain, retina and spinal cord (Fig. 1B). Notably, olfactory bulbs were frequently missing in the Tg brains in which Hes5 and GFP were highly expressed (Fig. 1B, arrows). We confirmed by *in situ* hybridization that *Hes5* expression was enhanced in the ventricular zone (VZ) and subventricular zone (SVZ), in which GFP was highly expressed (Fig. 1C). Real-time RT-PCR revealed that expression of *Hes5* mRNA increased by E10.5 when Dox was administered starting at E9.5 (Fig. 1D). GFP overlapped with Pax6, a marker for NSCs, and partially overlapped with Tbr2, a marker for intermediate progenitor cells (IPs), and Tuj1, a neuronal marker, in the dorsolateral telencephalon (neocortical regions) (Fig. 1E). Noticeably, the lateral ventricles and the VZ ($Pax6^+$) were dilated, and the thicknesses of neuronal layers ($Tuj1^+$) were markedly thinner in the Tg brain compared to the WT brain (Fig. 1F). $Tbr2^+$ IPs in the SVZ were reduced in number, and the thickness of the cortical plate (CP), which consists of $NeuN^+$ differentiated neurons, was also reduced in the Tg brain at all developmental stages examined (Fig. 1G-J), indicating that Hes5 overexpression led to maintenance and expansion of NSCs by inhibiting neuronal differentiation. However, analysis of neurogenesis/gliogenesis at postnatal stages was difficult because the Tg mice could not survive after birth, although the cause of death is unknown.

Hes5 overexpression suppressed proliferation of neural progenitors

Although neuronal differentiation was inhibited and NSCs were maintained longer in the Tg brain, the brain size was rather reduced (Fig. 1B). Therefore, we analyzed cell death and cell proliferation activity in neural progenitors in the neocortical regions. Immunostaining with anti-cleaved caspase-3 antibodies revealed that cell death was slightly enhanced in the neocortical regions of Tg brain (Fig. S1A). Next, we assessed cell proliferation by conducting 5-bromo-2′-deoxyuridine (BrdU) incorporation experiments and immunostaining with antibodies against Ki67, a marker of proliferating cells, and phospho-histone H3 (pH3), a marker of dividing cells in M phase. BrdU was administered intraperitoneally to pregnant mice 30 min before sacrifice at E13.5 or E15.5 to mark cells that incorporated BrdU in S phase. Although the number of $Ki67^+$ cells was rather increased in the Tg brain at E13.5, $BrdU^+$ and $pH3^+$ cells were decreased in number in the neocortical regions of Tg brain compared to WT brain (Fig. S1B). Later, at E15.5, the numbers of $BrdU^+$ and $pH3^+$ cells were markedly reduced in the neocortical regions of Tg brain compared to WT brain (Fig. S1C), indicating that proliferating cells and dividing cells were reduced in number in the Tg brain. These results suggested that cell proliferation activity was suppressed by Hes5 overexpression, thus leading to unexpectedly smaller brain size in the Tg mice. Next, we analyzed self-renewal versus cell cycle exit of NSCs in the WT and Tg brains. We administered 5-ethynyl-2′-deoxyuridine (EdU) intraperitoneally to pregnant mice at E14, and characterized EdU^+ cells by immunostaining with anti-Pax6, Tbr2, Tuj1 and Ki67 antibodies 12 h later at E14.5. A higher proportion of EdU-incorporated cells remained as $Pax6^+$ NSCs in the Tg brain compared to the WT brain (Fig. S2A,B), whereas more EdU^+ cells were colabeled with Tbr2 and Tuj1 in the WT brain than in the Tg brain (Fig. S2C-F). In line with these observations, the proportion of $Ki67^+;EdU^+/EdU^+$ (cell cycle re-entry) was higher in the Tg cortex, whereas the proportion of $Ki67^-;EdU^+/EdU^+$ (cell cycle exit) was higher in the WT cortex at E14.5 (Fig. S2G,H). Taken together, these results indicated that the frequency of self-renewal of NSCs was higher in the Tg cortex than in the WT cortex.

The thicknesses of all cortical layers were reduced in the Tg cortex

Next, we analyzed the expression of Hes1 and neurogenic bHLH genes such as *Neurog2* and *Ascl1*. Expression levels of Hes1 (protein and mRNA) and *Neurog2* mRNA were downregulated in the VZ of neocortical regions of Tg brain (Fig. 2A,B), while *Ascl1* expression in the neocortical regions was not significantly altered, indicating that Hes5 overexpression could repress *Neurog2* and inhibit neuronal differentiation even when Hes1 activity was attenuated. This result is consistent with the notion that Hes1 and Hes5 show compensatory expression patterns in the developing nervous system through mutual repression of their transcription (Hatakeyama et al., 2004). In addition, we found that the thicknesses of all cortical layers were reduced in the Tg brain by using markers for layers II-IV (Cux1), layer V (Ctip2) and layer VI (Tbr1) neurons at E15.5 and postnatal day 0 (P0) (Fig. 2C-E). Furthermore, reduction in the expression level of *Fezf2*, a fate determinant of $Ctip2^+$ neurons, which correspond to subcerebral projection neurons (SCPNs), was demonstrated by *in situ* hybridization (Fig. 2F). Real-time RT-PCR using total RNAs prepared from the neocortical regions revealed that expression levels of *Tbr1*, *Ctip2* (*Bcl11b* – Mouse Genome Informatics) and *Fezf2* were significantly downregulated in the Tg brain at E14.5 and E16.5 (Fig. 2G). However, *Cux1* expression was not significantly changed, probably because it was maintained in the VZ/SVZ (Fig. 2C). It is likely that the suppressed proliferation of neural progenitors via Hes5 overexpression led to the reduced thicknesses of all cortical layers and smaller brain size in the Tg mice.

Switching from deep to superficial layer neurogenesis precociously occurred in the Tg mice

Next, we performed birth-date analysis by administering EdU intraperitoneally to pregnant mice. When EdU was injected at E10.5, more EdU^+ cells, which were born during the period of EdU exposure, were found as layer VI neurons ($Tbr1^+$) in the Tg cortex at E18.5, suggesting an earlier onset of neurogenesis in the Tg brain compared to the WT brain (Fig. S3A,B). When EdU was administered at E11.5, most EdU^+ cells were located in layer VI ($Tbr1^+$) of the WT brain, while more EdU^+ cells were observed in layer V ($Ctip2^+$) of the Tg brain compared to the WT brain (Fig. S3C-F). When EdU was injected at E12.5, most EdU^+ neurons were still located in layer VI ($Tbr1^+$) but not in layer V ($Ctip2^+$) of the WT cortex at E18.5 (Fig. 3A,B). By contrast, EdU^+ cells were distributed in layer VI ($Tbr1^+$), layer V ($Ctip2^+$), and further upper layers of the Tg cortex, suggesting that $Ctip2^+$ layer V and further upper layer neurons were born prematurely in the Tg brain. In the WT brain, when EdU was injected at E13.5, the majority of EdU^+ cells were located in layer V ($Ctip2^+$), while some were in layers

Development (2017) 144, 3156-3167 doi:10.1242/dev.147256

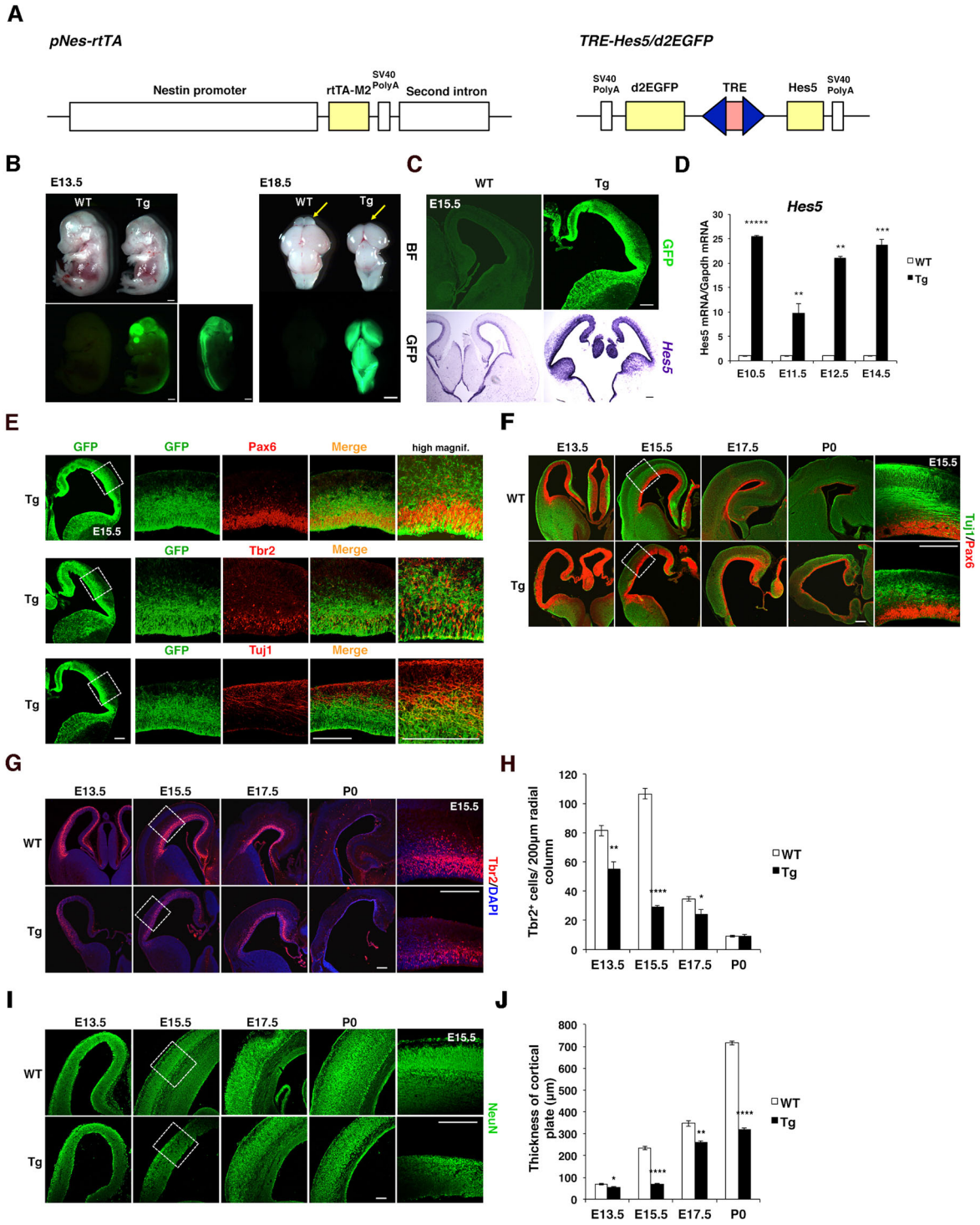

Fig. 1. Brain morphology of Hes5-overexpressing Tg mice. (A) Structure of *pNes-rtTA* and *TRE-Hes5/d2EGFP* transgenes. (B) Comparison of whole body (E13.5) and brain (E18.5) shape of WT and Hes5-overexpressing Tg mice. Dox was administered from E9.5 onward. GFP expression was detected throughout the CNS under a fluorescent microscope. Note that the olfactory bulbs were missing in the Tg brain (arrows), in which Hes5 and GFP were highly expressed. (C) Immunohistochemistry using anti-GFP antibodies to detect GFP (green), and *in situ* hybridization for *Hes5* mRNA expression (purple), in coronal sections of the WT and Tg telencephalon at E15.5. (D) Quantitative real-time RT-PCR using total RNAs prepared from the telencephalon of WT and Tg embryos at the indicated stages. Dox was administered from E9.5 onward. *Gapdh* was used as an internal control, and the values were normalized to that of the WT sample at each stage. (E) Characterization of Hes5/d2EGFP-expressing cells. Coronal sections of the neocortical regions of E15.5 Tg embryos were double stained using anti-GFP (green) and anti-Pax6/Tbr2/Tuj1 (red) antibodies. The boxed areas are magnified in the right panels, and merged images are further magnified in the rightmost panels. (F) Tuj1 (green) and Pax6 (red) staining in coronal sections of the WT and Tg telencephalon at various developmental stages. (G,H) Tbr2 staining (red) in coronal sections of the WT and Tg telencephalon at the indicated stages (G), and quantification of $Tbr2^+$ cell number in a radial column of 200 μm width in the neocortical regions (H). DAPI (blue) was used for nuclear staining. (I,J) NeuN staining (green) in coronal sections of the neocortical regions at the indicated stages (I), and quantification of the thickness of CP ($NeuN^+$) (J). (F,G,I) The boxed areas in photos at E15.5 are magnified in the rightmost panels. (D,H,J) Data are mean±s.e.m. (n=3); **P*<0.05, ***P*<0.01, ****P*<0.001, *****P*<0.0001, ******P*<0.00001 (Student's *t*-test). Scale bars: 1 mm in B; 200 μm in C, E, F, G and I.

Development (2017) 144, 3156-3167 doi:10.1242/dev.147256

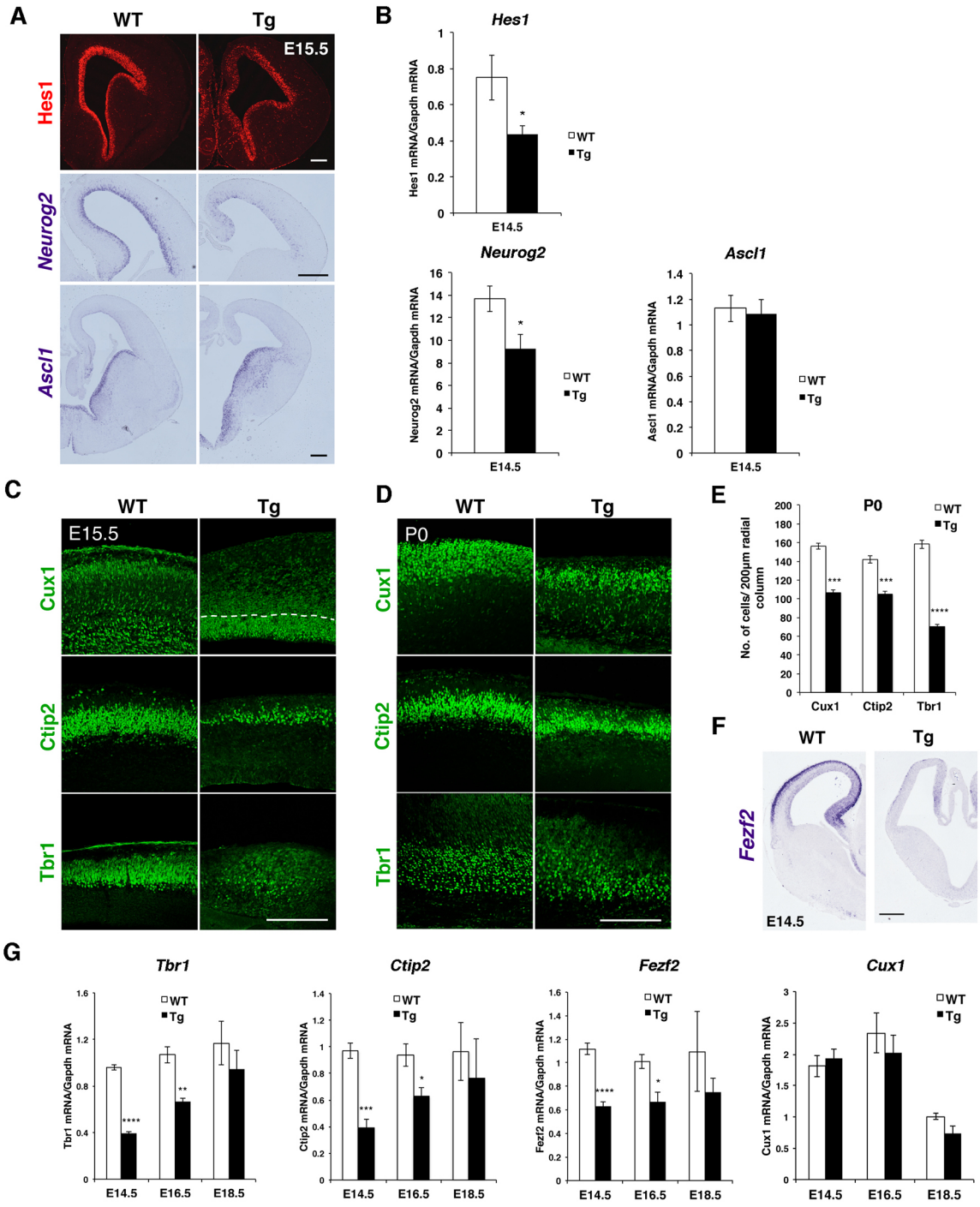

Fig. 2. Expression of neurogenic bHLH genes and generation of layer-specific neurons. (A) Immunohistochemistry for the bHLH repressor Hes1 (red), and *in situ* hybridization for mRNA expression of the neurogenic bHLH genes *Neurog2* and *Ascl1* (purple), in coronal sections of the telencephalon of WT and Hes5-overexpressing Tg mice at E15.5. (B) Quantitative real-time RT-PCR using total RNAs prepared from the neocortical regions of WT and Tg embryos at E14.5. *Gapdh* was used as an internal control. (C,D) Immunohistochemistry using layer-specific markers (Cux1 for layers II-IV, Ctip2 for layer V, and Tbr1 for layer VI) in coronal sections of the neocortical regions at E15.5 (C) and P0 (D). The border between the VZ and SVZ is indicated by a dotted line. (E) Graphs showing the numbers of Cux1$^+$, Ctip2$^+$ and Tbr1$^+$ cells in a radial column of 200 µm width at P0. (F) *In situ* hybridization for mRNA expression of *Fezf2* in coronal sections of the WT and Tg telencephalon at E14.5. (G) Real-time RT-PCR using total RNAs prepared from the neocortical regions of WT and Tg embryos at E14.5, E16.5 and E18.5. Expression levels of *Tbr1*, *Ctip2*, *Fezf2* and *Cux1* were compared between WT and Tg brains. *Gapdh* was used as an internal control. (B,E,G) Data are mean±s.e.m. (n=3); *P<0.05, **P<0.01, ***P<0.001, ****P<0.0001 (Student's t-test). Scale bars: 200 µm.

II-IV (Cux1$^+$) (Fig. 3C,D). By contrast, in the Tg brain, the majority of EdU$^+$ cells were distributed in layers II-IV (Cux1$^+$), while some were in layer V (Ctip2$^+$), suggesting that Cux1$^+$ layer II-IV neurons were born prematurely in the Tg brain. When EdU was injected at E14.5, most EdU$^+$ cells were settled in layers II-IV (Cux1$^+$) of both WT and Tg brains (Fig. 3E,F). These results indicated that Hes5 overexpression accelerated the switching from deep to superficial layer neurogenesis.

Development (2017) 144, 3156-3167 doi:10.1242/dev.147256

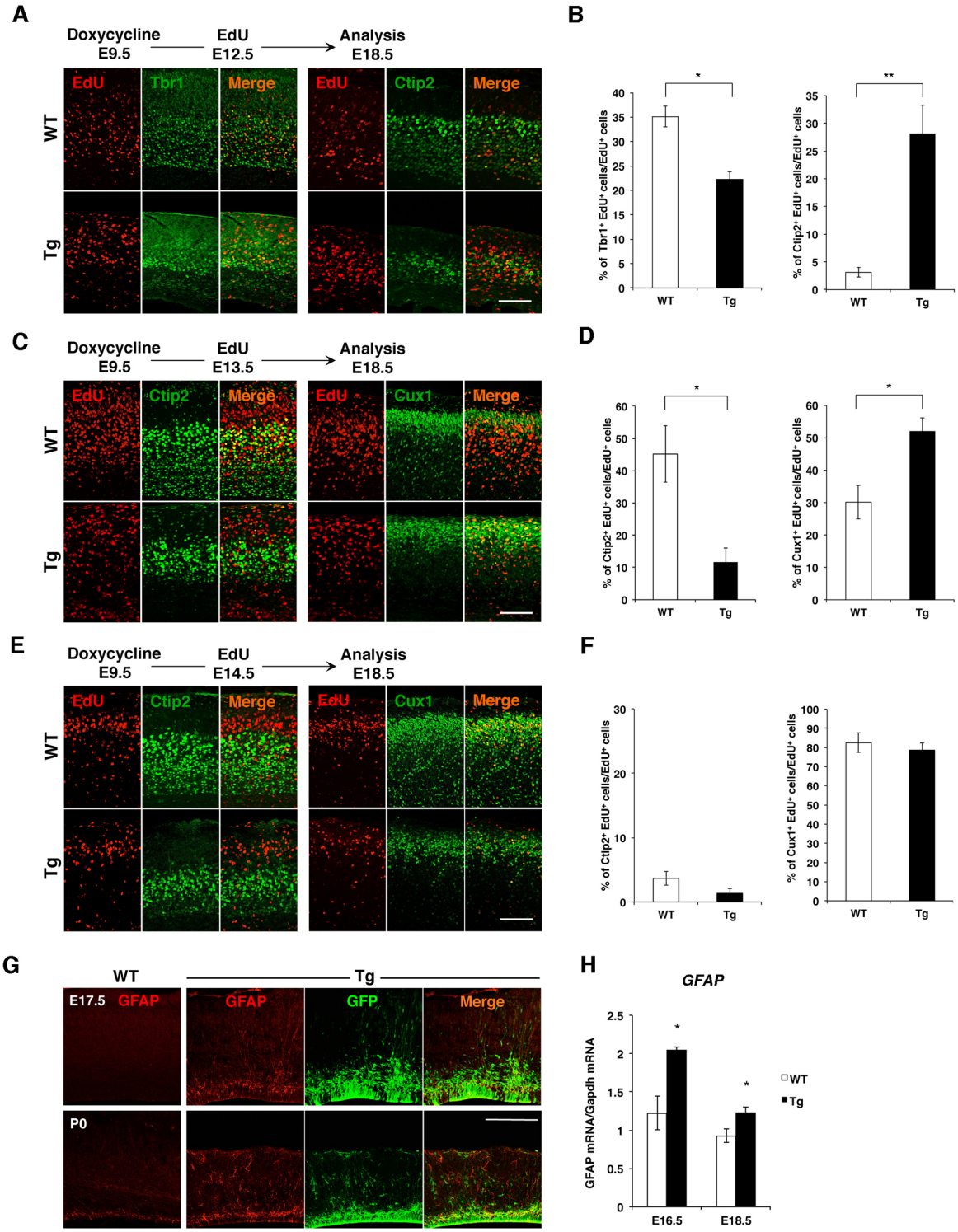

Fig. 3. Analyses of the transition timing of layer-specific neurogenesis and gliogenesis in the Hes5-overexpressing Tg brain. (A,C,E) Birth-date analysis of cortical neurons in WT and Tg brains. EdU was administered at E12.5 (A), E13.5 (C) or E14.5 (E), and the locations and fates of EdU-incorporated cells (red) were examined by the layer-specific markers Tbr1/Ctip2/Cux1 (green) at E18.5. (B,D,F) Graphs showing the proportions of each layer-specific neurons among EdU$^+$ cells. Total numbers of EdU$^+$ cells counted for the quantification were ≥100 cells for each analysis. (G) Analysis of generation of astrocytes in the neocortical regions of WT and Tg brains at E17.5 and P0. Double staining was performed using anti-GFAP (red) and anti-GFP (green) antibodies in coronal sections. (H) Real-time RT-PCR for *GFAP* expression using total RNAs prepared from the neocortical regions of WT and Tg brains at E16.5 and E18.5. *Gapdh* was used as an internal control. (B,D,F,H) Data are mean±s.e.m. (n=3); *P<0.05, **P<0.01 (Student's t-test). Scale bars: 200 µm.

Astrogenesis was accelerated and enhanced in the Tg brain

We next addressed whether the onset of gliogenesis was likewise accelerated in the neocortical regions by Hes5 overexpression. Although expression of GFAP (a marker for astrocytes) was not observed in the neocortical regions of WT mice at E17.5, a considerable number of GFAP$^+$ astrocytes precociously appeared in

Development (2017) 144, 3156-3167 doi:10.1242/dev.147256

the neocortical regions of Tg mice (Fig. 3G). Whereas GFAP signal was present in the neocortical regions of WT mice at P0, the number of GFAP$^+$ astrocytes was markedly higher in the VZ/SVZ and throughout the cortex of Tg mice. Most GFAP$^+$ cells coexpressed GFP in the VZ/SVZ, but many GFAP$^+$ cells in the outer region were GFP$^-$, suggesting that the outer region GFAP$^+$ cells lost Hes5/d2EGFP expression over the course of glial differentiation. Real-time RT-PCR demonstrated that *GFAP* expression was significantly higher in the neocortical regions of Tg brain at E16.5 and E18.5 (Fig. 3H). These results indicated that astrogenesis was accelerated and enhanced by Hes5 overexpression. In addition, we analyzed the generation of oligodendrocyte lineage cells with antibodies against Olig2, a marker for oligodendrocytes, and found that the numbers of Olig2$^+$ cells were reduced in the neocortical regions of Tg brain compared to WT brain at E17.5 and E18.5 (Fig. S4). This might be attributed to the hypoplastic ventral telencephalon (Fig. 1F), which is the primary source of oligodendrocyte progenitor cells.

Transition timing of layer-specific neurogenesis and astrogenesis was delayed in the absence of *Hes5*

Subsequently, we performed birth-date analysis in the neocortical regions of *Hes5* KO mice (Ohtsuka et al., 1999; Hatakeyama et al., 2004). When EdU was injected at E10.5 or E11.5, we did not find any significant difference in early neurogenesis between the WT and KO mice (data not shown). However, when EdU was injected at E14.5, most EdU$^+$ cells were located in layers II-IV (Cux1$^+$), but not in layer V (Ctip2$^+$), of the WT cortex, whereas EdU$^+$ cells were predominantly distributed in layer V (Ctip2$^+$), and fewer EdU$^+$ cells were located in layers II-IV (Cux1$^+$) of the *Hes5* KO cortex, at E18.5 (Fig. 4A,B), indicating that the switching from deep to superficial layer neurogenesis was delayed in the *Hes5* KO brain. In addition, immunohistochemistry and real-time RT-PCR for GFAP expression revealed the delayed onset of astrogenesis in the neocortical regions of *Hes5* KO brain compared to WT brain at E18.5 (Fig. 4C,D). These results exhibited striking contrast to the accelerated neurogenesis and astrogenesis observed in the Hes5-overexpressing Tg mice.

Hmga genes were downregulated by overexpression of Hes5

Because it has been found that PcG complex and Hmga proteins govern the developmental timing of neurogenesis and gliogenesis, we assessed their expression levels in the Hes5-overexpressing Tg brain. Real-time RT-PCR demonstrated upregulation of *Ezh2* and *Eed*, components of polycomb repressive complex 2 (PRC2), in the neocortical regions of Tg brain at E12.5 (Fig. 5A), whereas the expression of *Ring1B* (*Rnf2* – Mouse Genome Informatics), a

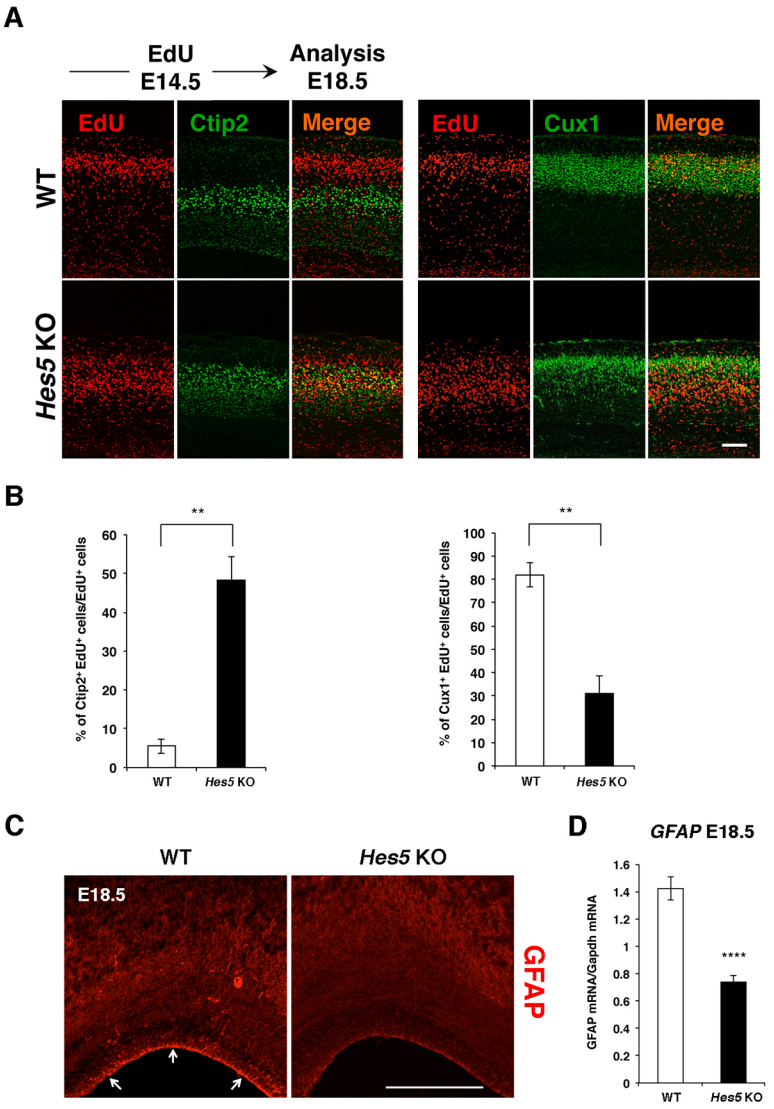

Fig. 4. Estimation of the transition timing of neurogenesis and astrogenesis in *Hes5* KO mice. (A) Birth-date analysis in the neocortical regions of WT and *Hes5* KO brains. EdU was administered at E14.5, and the locations and fates of EdU-incorporated cells (red) were examined by the layer-specific markers Ctip2 and Cux1 (green) at E18.5. (B) Graphs showing the proportions of Ctip2$^+$ cells and Cux1$^+$ cells among EdU$^+$ cells. Total numbers of EdU$^+$ cells counted for the quantification were ≥100 cells for each analysis. (C) Analysis of generation of astrocytes using anti-GFAP antibodies (red) in the neocortical regions of WT and *Hes5* KO brains at E18.5. Arrows indicate GFAP expression in the VZ. (D) Real-time RT-PCR for mRNA expression of *GFAP* using total RNAs prepared from the neocortical regions of WT and KO brains at E18.5. *Gapdh* was used as an internal control. (B,D) Data are mean±s.e.m. (n=4); **P<0.01, ****P<0.0001 (Student's t-test). Scale bars: 200 µm.

Development (2017) 144, 3156-3167 doi:10.1242/dev.147256

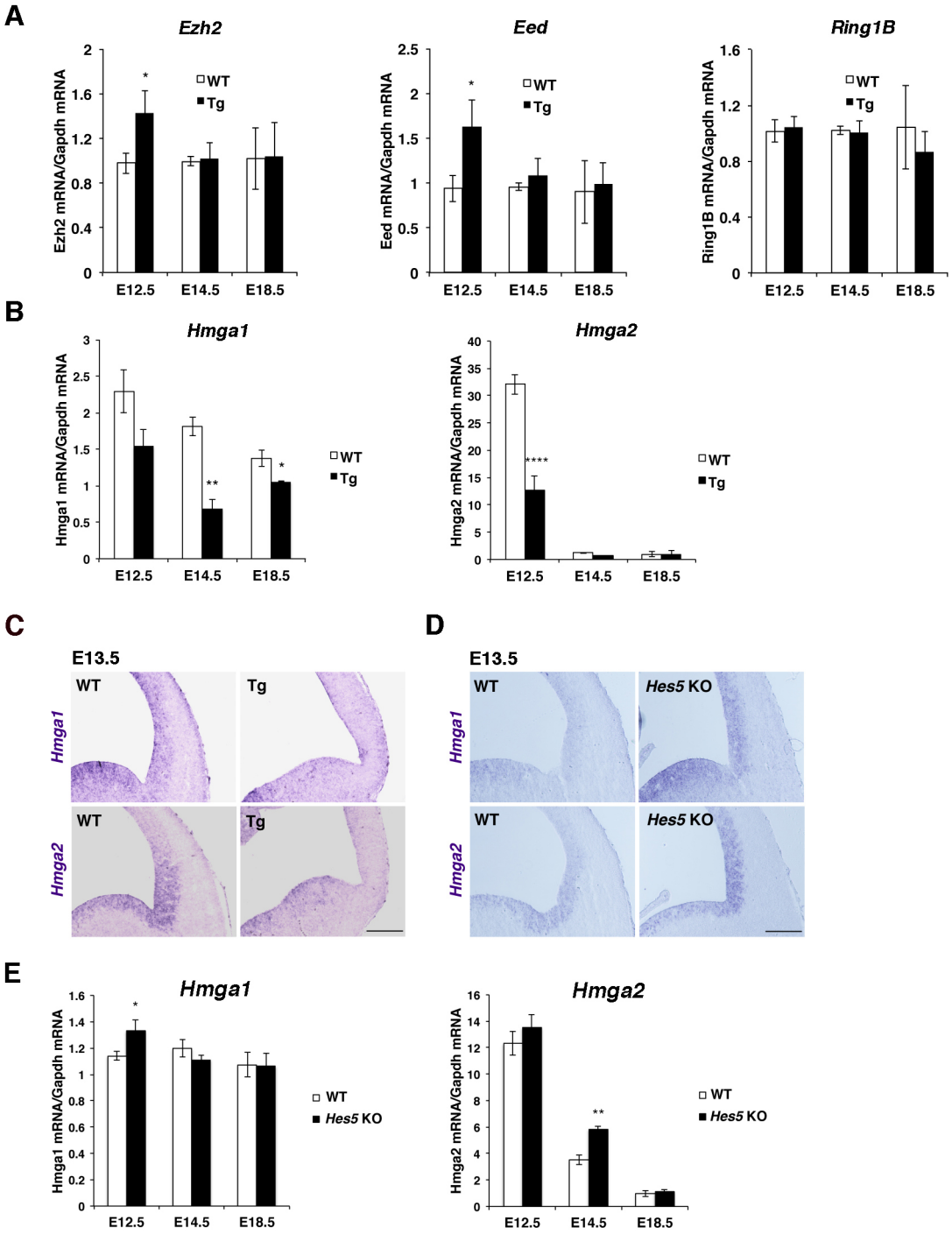

Fig. 5. Altered expression levels of *Hmga1/2* in the neocortical regions. (A,B) Real-time RT-PCR using total RNAs prepared from the neocortical regions of WT and Hes5-overexpressing Tg brains. mRNA levels of PcG components, such as *Ezh2*, *Eed* and *Ring1B* (A), and *Hmga1 and Hmga2* (B), were quantified at E12.5, E14.5 and E18.5. (C,D) *In situ* hybridization for *Hmga1* and *Hmga2* mRNA expression in coronal sections of WT versus Hes5-overexpressing Tg brains (C), and WT versus *Hes5* KO brains (D), at E13.5. Note that the color development time was shorter for the data in D than in C. (E) Real-time RT-PCR for *Hmga1 and Hmga2* using total RNAs prepared from the neocortical regions of WT and *Hes5* KO brains at E12.5, E14.5 and E18.5. (A,B,E) *Gapdh* was used as an internal control. Data are mean±s.e.m. (n=3); *P<0.05, **P<0.01, ****P<0.0001 (Student's t-test). Scale bars: 200 µm.

component of PRC1, was not significantly affected. *In situ* hybridization also demonstrated a subtle increase in the expression levels of both genes in the neocortical regions of Tg brain at E12.5 (Fig. S5A,B). Notably, expression levels of *Hmga1* and *Hmga2* were significantly reduced in the Tg brain compared to the WT brain (Fig. 5B). We confirmed by *in situ* hybridization that the expression of both *Hmga1* and *Hmga2* was remarkably downregulated in the neocortical regions of Tg brain compared to WT brain (Fig. 5C). Conversely, expression levels of *Hmga1* and *Hmga2* were upregulated in the neocortical regions of *Hes5* KO brain compared to WT brain (Fig. 5D,E). Expression levels of *Hmga1/2* in the ventral telencephalon, diencephalon, midbrain and hindbrain were not much altered in the Tg brain, although the brain shape was apparently deformed compared to that of the WT

Development (2017) 144, 3156-3167 doi:10.1242/dev.147256

(Fig. S5C,D). To reveal that the phenotype of *Hes5* KO brain is mediated by the upregulation of *Hmga1/2*, we performed knockdown experiments by introducing a combination of expression vectors of shRNA targeting *Hmga1* (*shHmga1*) and *Hmga2* (*shHmga2*), in addition to scrambled shRNA control vectors (*shScrambled*) (Kishi et al., 2012), in the VZ of the KO brain by *in utero* electroporation at E13.5. When we performed birth date analysis of *Hmga1/2* knockdown cells by administering EdU at E14.5, the switching delay was partially recovered by *Hmga1/2* knockdown in the *Hes5* KO brain (Fig. 6). Taken together, these results suggest that the transition timing of layer-specific neurogenesis and astrogenesis was regulated at least partly by the expression levels of *Hmga1/2* genes.

Hes5 repressed the promoter activity of Hmga genes

We next conducted reporter analysis using the *Hmga1* (−5000 to +28) and *Hmga2* (−3111 to +56) promoters to test whether Hes5 downregulates the transcription of these genes (Fig. 7A). Cotransfection of Hes5 expression vectors (*pEF-HA-Hes5*) with reporter vectors (*pHmga1-luc* or *pHmga2-luc*) in NIH3T3 cells or mouse neural stem (NS) cells significantly downregulated the promoter activity of both *Hmga1* and *Hmga2* in a dose-dependent manner (Fig. 7B), suggesting that Hes5 functions as a negative regulator for transcription of *Hmga1/2*. Because the promoter activity of *Hmga1* was more effectively downregulated by Hes5 expression compared to that of *Hmga2*, we focused on the *Hmga1* promoter for further analysis. We narrowed down the promoter sequence to the regions responsible for the Hes5-mediated transcriptional repression. Intriguingly, the promoter regions 2.5 kb and 3.9 kb upstream of the ATG codon exhibited no apparent repression by Hes5, whereas the 4.6 kb promoter region exhibited Hes5-mediated transcriptional repression (Fig. 7C,D), suggesting that the specified region (between −4596 and −3910) and/or surrounding region contains critical regulatory sites. It has been established that the Hes family of bHLH factors repress transcription by binding to the N box (CACNAG) and the class C site [CACG(C/A)G], and we found one N box (−4547 to −4542) within the specified region. Therefore, we constructed *Hmga1* reporter vectors with various modifications in the N box, such as substitutions of 1, 2 or 5 nucleotides, or a deletion of all six nucleotides in the N box sequence, and performed the luciferase assay. However, these modifications resulted in only mild effects on *Hmga1* promoter activity. Given that there are many N box/class C sites in the *Hmga1* promoter, as shown in Fig. 7C, it is possible that modifications in a few N box/class C sites cannot induce an effective de-repression. In addition, we found several E box sequences in the *Hmga1* promoter region, suggesting that the *Hmga1* transcriptional activity could be indirectly regulated by Hes5 through other regulatory sequences including E box.

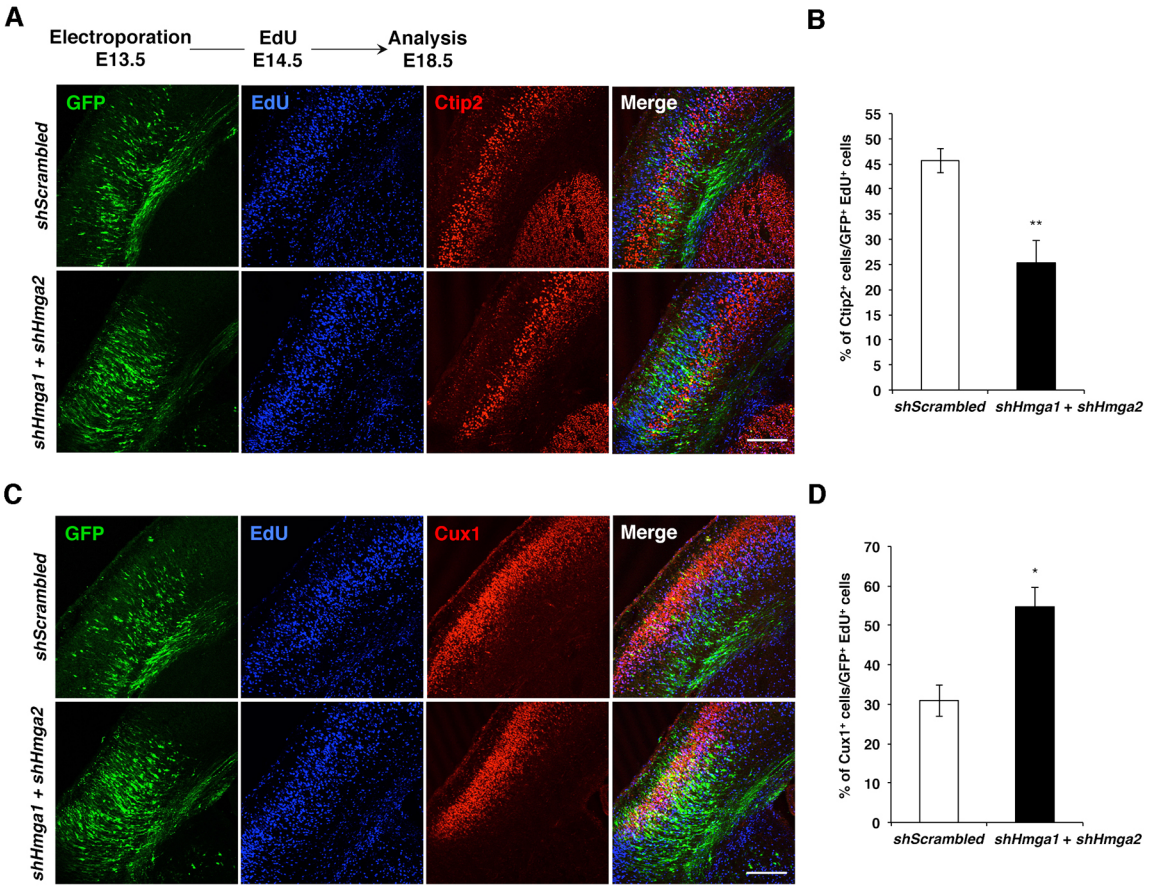

Fig. 6. Knockdown experiments for *Hmga1/2* in the *Hes5* KO cortex. (A,C) Birth-date analysis of *Hmga1/2* knockdown cells in the cortex of *Hes5* KO brain. Control vectors (*shScrambled*) or a combination of *Hmga1/2* knockdown vectors (*shHmga1* and *shHmga2*) together with *pEF-EGFP* vectors were introduced into the VZ cells by *in utero* electroporation at E13.5. EdU was administered at E14.5, and the locations and fates of newly born neurons that coexpressed GFP (green) and EdU (blue) were examined by the layer-specific markers Ctip2 (A, red) and Cux1 (C, red) at E18.5. (B,D) Graphs showing the proportions of $Ctip2^+$ cells (B) and $Cux1^+$ cells (D) among cells colabeled with GFP and EdU. Total numbers of EdU^+ cells counted for the quantification were ≥100 cells for each analysis. Data are mean±s.e.m. (n=3); *P<0.05, **P<0.01 (Student's t-test). Scale bars: 200 µm.

Development (2017) 144, 3156-3167 doi:10.1242/dev.147256

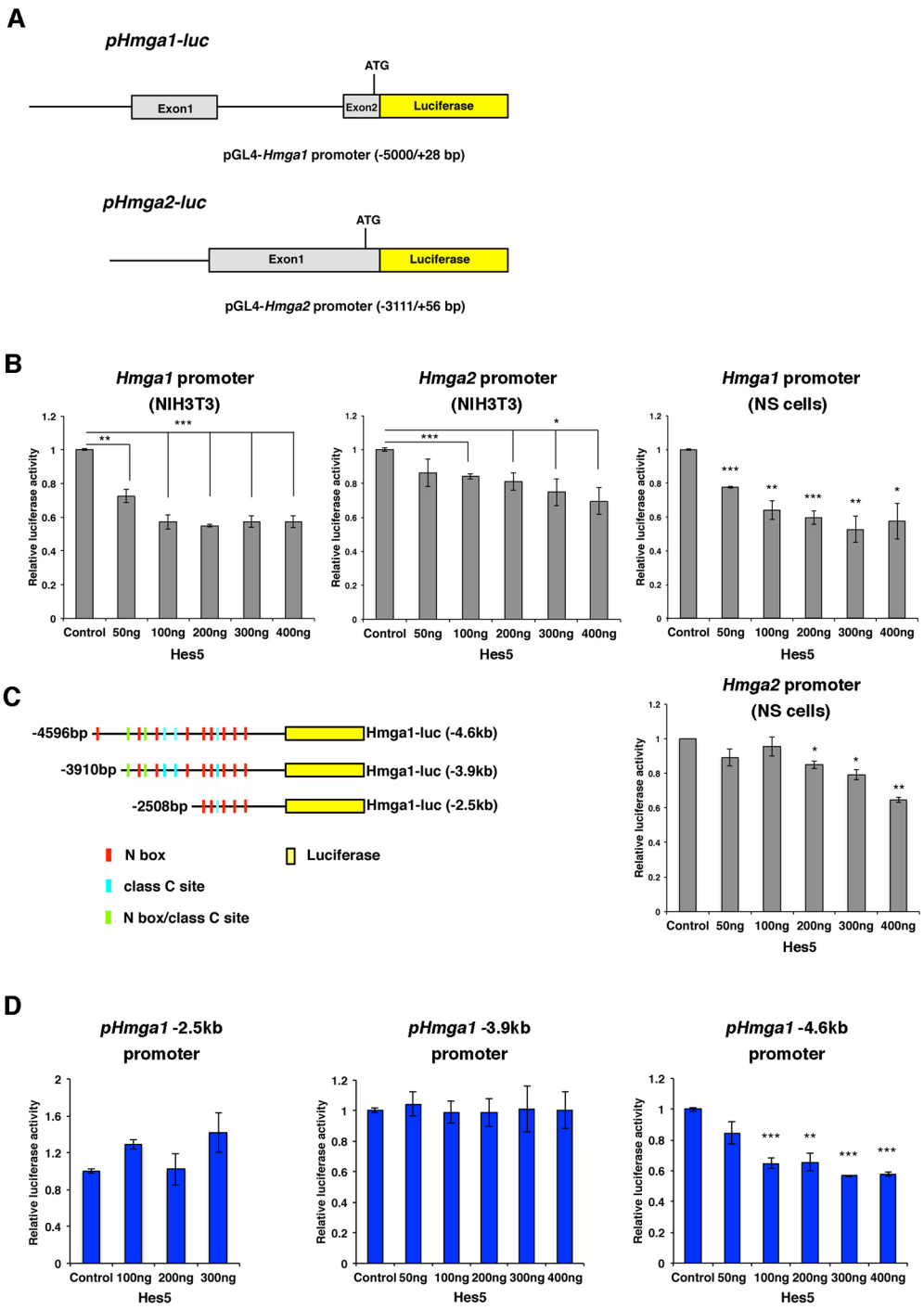

Fig. 7. Reporter analysis using the promoters of *Hmga1/2*. (A) Constructs of reporter vectors containing the promoter regions of *Hmga1/2*. *Hmga1* (*variant 1*) promoter region (from −5000 to +28) or *Hmga2* promoter region (from −3111 to +56) was cloned into the luciferase vector *pGL4.10*. (B) Luciferase reporter assay using various amounts of Hes5 expression vector (*pEF-HA-Hes5*). Vectors were cotransfected in NIH3T3 cells or mouse NS cells, and the luciferase activity was measured 24 h later. (C) Truncated promoter regions of the *Hmga1* gene used for the reporter assay. Locations of the putative N box (CACNAG), the class C sites [CACG(C/A)G], and N box/class C sites are indicated by red, blue and green lines, respectively. (D) Reporter assay using various amounts of Hes5 expression vector with truncated versions of *Hmga1* reporter vectors. Vectors were cotransfected in NIH3T3 cells and the luciferase activity was measured 24 h later. (B,D) Values were normalized to those of the control samples. Data are mean±s.e.m. (*n*=3); **P*<0.05, ***P*<0.01, ****P*<0.001 (Student's *t*-test).

DISCUSSION

Hes5 expression leads to suppression of the promoter activity of Hmga and regulates the transition timing of neocortical neurogenesis and gliogenesis

In the present study, we showed that the transition timing from deep to superficial layer neurogenesis was shifted earlier and gliogenesis was also accelerated with an earlier termination of the neurogenic period via overexpression of Hes5 (Fig. 3); conversely, the transition from deep to superficial layer neurogenesis and the onset of gliogenesis were delayed in *Hes5* KO mice (Fig. 4). These results suggest that these transitions are not governed by the number of cell divisions, given that the cell cycle progression was slower in NSCs in the neocortical regions of the Tg brain (Fig. S1), which is in line with a previous report that the transition in temporal identity of NSCs can be controlled independently of cell cycle (Okamoto et al., 2016). Therefore, we next addressed whether the machinery that regulates the transition timing of neurogenesis and gliogenesis was affected by Hes5 overexpression.

Temporal modification of the chromatin structure by the PcG complex is known to be one of the key mechanisms regulating the transition timing of neocortical neurogenesis and gliogenesis (Vogel et al., 2006; Hirabayashi et al., 2009; Pereira et al., 2010; Morimoto-Suzki et al., 2014; Corley and Kroll, 2015). It is also known that there are two classes of PRC; PRC1 contains a ubiquitin ligase Ring1A/B and PcG RING finger (PCGF) proteins, and PRC2 is composed of Eed, Suz12 and a methyltransferase Ezh1/2 (Schwartz and Pirrotta,

Development (2017) 144, 3156-3167 doi:10.1242/dev.147256

2013). Morimoto-Suzki et al. reported that Ring1B suppresses Fezf2, a fate determinant of Ctip2^{+} SCPNs [a class of deep layer (layer V) neurons], and has a role in terminating the generation of Ctip2^{+} neurons (Morimoto-Suzki et al., 2014). These findings suggested that Ring1B mediates the timed termination of Fezf2 expression and switching from deep to superficial layer neurogenesis. Hirabayashi et al. reported that the level of H3K27me3 at the *Neurog1* promoter region gradually increases over time, and that PcG proteins suppress the *Neurog1* locus during the astrogenic phase and mediate the neurogenic-to-gliogenic fate switching in the developing cortex (Hirabayashi et al., 2009). In the present study, expression levels of *Ezh2* and *Eed* were upregulated by Hes5 overexpression in the neocortical regions only during the early neurogenic stages (Fig. 5A). By contrast, expression levels of *Hmga1/2* were markedly downregulated in the neocortical regions of Hes5-overexpressing Tg brain, but upregulated in the *Hes5* KO brain (Fig. 5C-E).

Hmga proteins belong to the Hmg protein family, which consists of nonhistone chromatin-associated proteins that regulate gene expression by modulating chromatin structure (Ozturk et al., 2014). Among their diverse functions, previous reports have uncovered roles in self-renewal of NSCs (Nishino et al., 2008) and gliogenesis during brain development (Sanosaka et al., 2008). It was revealed that Hmga2 promotes self-renewal of NSCs by decreasing p16^{Ink4a}/p19^{Arf} expression, but its expression declines with age, partly due to the increasing expression of *let-7b* microRNA (Nishino et al., 2008). Furthermore, it has been reported that Hmga proteins are essential for the open chromatin state in early-stage NSCs to maintain their neurogenic potential at early developmental stages (Kishi et al., 2012). Overexpression of Hmga proteins can retrieve the neurogenic potential even in late-stage NSCs, and knockdown of *Hmga1/2* promotes astrogenesis. In addition, Fujii et al. reported that insulin-like growth factor 2 mRNA-binding protein 2 (Igf2bp2) is one of the key mediators of Hmga function that regulates the neurogenic potential of early-stage NSCs (Fujii et al., 2013). Thus, it is likely that the downregulation of *Hmga1/2* accelerated the transition from deep to superficial layer neurogenesis and the onset of astrogenesis in the Hes5-overexpressing Tg cortex. This accelerated transition might be partly due to the higher activity of PcG complexes (Fig. 5A), which might have caused the reduction in *Fezf2* expression (Fig. 2F,G), resulting in earlier termination of the generation of Ctip2^{+} deep layer neurons with precocious switching to production of Cux1^{+} superficial layer neurons (Fig. 3) in the Tg cortex. In the present study, we demonstrated that Hes5 expression leads to suppression of the promoter activity of *Hmga1/2* in reporter analyses (Fig. 7), although we could not obtain evidence for the direct regulation of *Hmga1/2* by Hes5. Likewise, we could not demonstrate the direct regulation of PcG genes, such as *Ezh2*, *Eed* and *Ring1B*, by Hes5 (data not shown), in agreement with the modest effects of Hes5 overexpression on expression levels of such PcG genes (Fig. 5A). However, it is possible that the activity of the PcG complex can be modulated by Hmga or other factors that are regulated by Hes5.

Precise control of Hes5 expression level is essential for normal neocortical development

During neocortical development, expression of Hes5 is upregulated after the onset of neurogenesis when NSCs start to receive strong intercellular Delta-Notch signals from differentiating and mature neurons (Hatakeyama et al., 2004). Our results indicate that the timing and levels of Hes5 expression must be properly regulated in order to maintain the precise temporal control of deep and superficial layer neurogenesis and switching from neurogenesis to gliogenesis in normal brain development. Otherwise, brain size and neocortical organization become disturbed. It has been revealed that Hes5 exhibits oscillatory expression in NSCs by a negative autoregulation mechanism (Imayoshi et al., 2013), similarly to Hes1 (Hirata et al., 2002), indicating the importance of the control of Hes5 expression within appropriate levels to avoid its excessive expression. Consistent with the above notion, we found that expression levels of *Hmga1/2* successively declined in NSCs of mouse neocortical regions during the mid-gestation period between E11.5 and E17.5, whereas *Hes5* expression was gradually upregulated during this period (Ohtsuka et al., 2011). Other research groups have also demonstrated that *HMGA2* expression successively decreased, while *HES5* expression gradually increased, in the developing human brain during the mid-gestation period (Patterson et al., 2014). Interestingly, Patterson et al. reported a link between the *let-7/HMGA2* circuit and Notch signaling. They found that HMGA2 regulated fate decisions between neurogenesis and gliogenesis in human NSCs via HES5, and that the *let-7* family of miRNAs downregulated *HMGA2* expression. In addition, they demonstrated that knockdown of *HMGA2* by small interfering RNA led to a dramatic downregulation of *HES5*, probably due to the blockade of access of NICD to the *HES5* promoter, while siRNA for *HES5* (40% knockdown of *HES5* expression) caused only a subtle increase in the *HMGA2* expression level. These results and the present findings together indicate a crucial correlation between downstream effectors of the Notch signaling pathway and epigenetic regulatory factors, although the entire mechanism and biological significance of the correlation between the two systems remain to be elucidated.

MATERIALS AND METHODS

Generation of transgenic mice

For the *pNes-rtTA* transgene, a *rtTA-Advanced* fragment excised from *pTet-On Advanced* vector (Clontech) was subcloned between the *Nes* promoter (5.8 kb) and polyadenylation sequence of *SV40* with the second intron (1.7 kb) of the *Nes* gene. For the *TRE-Hes5/d2EGFP* transgene, mouse *Hes5* and *d2EGFP* (Clontech) cDNAs were inserted into *pTRE-Tight-BI* vector (Clontech) (Fig. 1A). Two Tg mouse lines were generated using each transgene and maintained on the ICR background. Both lines were crossed and doxycycline hyclate (Sigma-Aldrich; 2.0 mg/ml) in drinking water with 5% sucrose was continuously administered to pregnant mice from E9.5 until sacrifice. Images of whole bodies with GFP fluorescence were obtained with a MZ16FA fluorescence stereo microscope equipped with a DFC300 FX digital camera (Leica). Animal experiments were carried out according to the guidelines for animal experiments at Kyoto University.

Immunohistochemistry

Immunohistochemistry was performed as described previously (Ohtsuka et al., 2011). Brains were fixed in 4% paraformaldehyde, incubated overnight with 20% (w/v) sucrose in PBS at 4°C, embedded in OCT compound and cryosectioned at 16 µm thickness. Sections were blocked with 5% normal goat serum in 0.1% Triton X-100 in PBS for 1 h at room temperature. Primary antibodies diluted in 1% normal goat serum/0.1% Triton X-100 in PBS were applied overnight at 4°C. Primary antibodies used in this study are listed in Table S1. Alexa Fluor-conjugated secondary antibodies (Molecular Probes; 1:200) were applied for 2 h at room temperature to detect primary antibodies. DAPI (4′,6-diamidino-2-phenylindole) (Sigma-Aldrich) was used for nuclear staining. Images were analyzed using a LSM510 confocal microscope (Zeiss).

In situ hybridization

Preparation of digoxygenin-labeled RNA probes and *in situ* hybridization were performed as described previously (Ohtsuka et al., 2011). The coding sequences of *Hes5* (NM_010419.4), *Hes1* (NM_008235.2), *Neurog2*

Development (2017) 144, 3156-3167 doi:10.1242/dev.147256

(NM_009718.2), *Ascl1* (NM_008553.4), *Fezf2* (NM_080433.3), *Hmga1* (NM_016660.3), *Hmga2* (NM_010441.2), *Ezh2* (NM_007971.2) and *Eed* (NM_021876.3) were used as templates for the RNA probes.

Quantitative real-time RT-PCR

Total RNA was prepared from the neocortical regions of mouse brains (Ohtsuka et al., 2011). Reverse transcription was performed using total RNA as described previously (Tan et al., 2012). *Gapdh* was used as an internal control. PCR primers are listed in Table S2.

BrdU incorporation assay

BrdU (Sigma-Aldrich; 50 µg BrdU/g of body weight) was injected intraperitoneally to pregnant mice 30 min before sacrifice. The $BrdU^+$ cells were detected by immunohistochemistry as described previously (Tan et al., 2012).

EdU birthdating

EdU (Molecular Probes; 12.5 µg EdU/g of body weight) was injected intraperitoneally to pregnant mice at E12.5, E13.5 or E14.5, and the offspring were analyzed at E18.5. EdU-labeled cells were detected by a fluorogenic click reaction (Salic and Mitchison, 2008). The numbers of EdU-labeled cells positive and negative for the layer marker were manually counted in the immunostained sections, and the proportions of EdU-labeled cells positive for the layer marker among total EdU-labeled cells were calculated. At least three sections of three mice were used for quantification.

Knockdown experiment

Knockdown experiments were performed by introducing a combination of expression vectors of shRNA targeting *Hmga1* (*pSiren-EGFP-shHmga1*) and *Hmga2* (*pSiren-EGFP-shHmga2*), in addition to scrambled shRNA control vectors (*pSiren-EGFP-shScrambled*) (Kishi et al., 2012), in the VZ of *Hes5* KO brain by *in utero* electroporation at E13.5. *pSiren-EGFP-shHmga1*, *pSiren-EGFP-shHmga2* and *pSiren-EGFP-shScrambled* vectors were kindly provided by Dr Yusuke Kishi and Dr Yukiko Gotoh (The University of Tokyo). *In utero* electroporation was performed as described previously (Ohtsuka et al., 2011).

Plasmids

For the Hes5 expression vector (*pEF-HA-Hes5*), a hemagglutinin (HA)-tagged coding sequence of *Hes5* (NM_010419.4) was cloned into *pEF-MM* vector. For the luciferase reporter constructs (*pHmga1-luc* and *pHmga2-luc*), a 5.0-kb fragment of the *Hmga1* (*variant 1*) (NM_016660.3) promoter region (from −5000 to +28, relative to the ATG codon in exon 2) or a 3.2-kb fragment of the *Hmga2* (NM_010441.2) promoter region (from −3111 to +56, relative to the ATG codon in exon 1) was inserted into the multiple cloning site of the *pGL4.10* luciferase vector (Promega). For the truncated versions of *Hmga1* reporters, −4596 bp, −3910 bp, −2508 bp, −2000 bp, −1506 bp and −1003 bp upstream promoter regions relative to the ATG codon were cloned into the *pGL4.10* luciferase vector.

Cell culture and transfection

NIH3T3 cells were cultured in DMEM and 10% FBS. Neural stem (NS) cells were originally established from basal forebrain regions of perinatal mice (Imayoshi et al., 2013) and maintained using a NS cell culture method as described previously (Conti et al., 2005) with minor modifications. Briefly, NS cells were plated in serum-free medium (DMEM/F12) supplemented with 1% N2-MAX medium (R&D Systems), 1% Penicillin/Streptomycin (Nacalai), 10 ng/µl of both EGF and basic FGF (Invitrogen), and 4 µg/ml laminin (Sigma-Aldrich). For transfection, NIH3T3 cells or NS cells were cultured at subconfluence and transfected using ViaFect transfection reagent (Promega) according to the manufacturer's instructions.

Reporter assay

The luciferase reporters of *Hmga1* or *Hmga2* (*pHmga1-luc* or *pHmga2-luc*) (0.1 µg) and the Hes5 expression plasmids (*pEF-HA-Hes5*) (0.05-0.4 µg) were transfected into NIH3T3 cells or mouse NS cells along with *pRL-SV40* (Promega) to normalize the transfection efficiency. The luciferase assay was performed 24 h post-transfection as described previously (Sakamoto et al., 2003).

Statistical analysis

Each value was obtained from at least three independent samples. Statistical significance was evaluated by Student's *t*-test. Data are presented as mean± s.e.m.

Acknowledgements

We thank Hitoshi Miyachi for help with the generation of *pNes-rtTA* and *TRE-Hes5/d2EGFP* transgenic mice; Yusuke Kishi and Yukiko Gotoh for *pSiren-EGFP-shHmga1*, *pSiren-EGFP-shHmga2* and *pSiren-EGFP-shScrambled* vectors; and Hiromi Shimojo for technical instruction and critical discussion.

Competing interests

The authors declare no competing or financial interests.

Author contributions

Conceptualization: S.B., R.K., T.O.; Methodology: S.B., T.O.; Investigation: S.B., T.O.; Writing - original draft: T.O.; Supervision: R.K., T.O.; Funding acquisition: R.K., T.O.

Funding

This work was supported by Core Research for Evolutional Science and Technology [JPMJCR12W2 to R.K.], Grant-in-Aid for Scientific Research on Innovative Areas from the Ministry of Education, Culture, Sports, Science and Technology (MEXT) [16H06480 to R.K.], and Grant-in-Aid for Scientific Research from the Japan Society for the Promotion of Science (JSPS) [15H02349 to R.K.; 23500390 and 15K06773 to T.O.].

Supplementary information

Supplementary information available online at
http://dev.biologists.org/lookup/doi/10.1242/dev.147256.supplemental

References

Artavanis-Tsakonas, S., Rand, M. D. and Lake, R. J. (1999). Notch signaling: cell fate control and signal integration in development. *Science* **284**, 770-776.

Berezovska, O., McLean, P., Knowles, R., Frosh, M., Lu, F. M., Lux, S. E. and Hyman, B. T. (1999). Notch1 inhibits neurite outgrowth in postmitotic primary neurons. *Neuroscience* **93**, 433-439.

Conti, L., Pollard, S. M., Gorba, T., Reitano, E., Toselli, M., Biella, G., Sun, Y., Sanzone, S., Ying, Q.-L., Cattaneo, E. et al. (2005). Niche-independent symmetrical self-renewal of a mammalian tissue stem cell. *PLoS Biol.* **23**, e283.

Corley, M. and Kroll, K. L. (2015). The roles and regulation of Polycomb complexes in neural development. *Cell Tissue Res.* **359**, 65-85.

de la Pompa, J. L., Wakeham, A., Correia, K. M., Samper, E., Brown, S., Aguilera, R. J., Nakano, T., Honjo, T., Mak, T. W., Rossant, J. et al. (1997). Conservation of the Notch signalling pathway in mammalian neurogenesis. *Development* **124**, 1139-1148.

Fujii, Y., Kishi, Y. and Gotoh, Y. (2013). IMP2 regulates differentiation potentials of mouse neocortical neural precursor cells. *Genes Cells.* **18**, 79-89.

Gridley, T. (1997). Notch signaling in vertebrate development and disease. *Mol. Cell. Neurosci.* **9**, 103-108.

Hatakeyama, J., Bessho, Y., Katoh, K., Ookawara, S., Fujioka, M., Guillemot, F. and Kageyama, R. (2004). Hes genes regulate size, shape and histogenesis of the nervous system by control of the timing of neural stem cell differentiation. *Development* **131**, 5539-5550.

Hirabayashi, Y., Suzki, N., Tsuboi, M., Endo, T. A., Toyoda, T., Shinga, J., Koseki, H., Vidal, M. and Gotoh, Y. (2009). Polycomb limits the neurogenic competence of neural precursor cells to promote astrogenic fate transition. *Neuron* **63**, 600-613.

Hirata, H., Yoshiura, S., Ohtsuka, T., Bessho, Y., Harada, T., Yoshikawa, K. and Kageyama, R. (2002). Oscillatory expression of the bHLH factor Hes1 regulated by a negative feedback loop. *Science* **298**, 840-843.

Imayoshi, I., Isomura, A., Harima, Y., Kawaguchi, K., Kori, H., Miyachi, H., Fujiwara, T., Ishidate, F. and Kageyama, R. (2013). Oscillatory control of factors determining multipotency and fate in mouse neural progenitors. *Science* **342**, 1203-1208.

Ishibashi, M., Moriyoshi, K., Sasai, Y., Shiota, K., Nakanishi, S. and Kageyama, R. (1994). Persistent expression of helix-loop-helix factor HES-1 prevents mammalian neural differentiation in the central nervous system. *EMBO J.* **13**, 1799-1805.

Kageyama, R. and Ohtsuka, T. (1999). The Notch-Hes pathway in mammalian neural development. *Cell Res.* **9**, 179-188.

Kishi, Y., Fujii, Y., Hirabayashi, Y. and Gotoh, Y. (2012). HMGA regulates the global chromatin state and neurogenic potential in neocortical precursor cells. *Nat. Neurosci.* **15**, 1127-1133.

Kopan, R., Nye, J. S. and Weintraub, H. (1994). The intracellular domain of mouse Notch: a constitutively activated repressor of myogenesis directed at the basic helix–loop–helix region of MyoD. *Development* **120**, 2385-2396.

Development (2017) 144, 3156-3167 doi:10.1242/dev.147256

McConnell, S. K. (1989). The determination of neuronal fate in the cerebral cortex. *Trends Neurosci.* **12**, 342-349.

Morimoto-Suzki, N., Hirabayashi, Y., Tyssowski, K., Shinga, J., Vidal, M., Koseki, H. and Gotoh, Y. (2014). The polycomb component Ring1B regulates the timed termination of subcerebral projection neuron production during mouse neocortical development. *Development* **141**, 4343-4353.

Nishino, J., Kim, I., Chada, K. and Morrison, S. J. (2008). Hmga2 promotes neural stem cell self-renewal in young but not old mice by reducing p16Ink4a and p19Arf expression. *Cell* **135**, 227-239.

Ohtsuka, T., Ishibashi, M., Gradwohl, G., Nakanishi, S., Guillemot, F. and Kageyama, R. (1999). Hes1 and Hes5 as notch effectors in mammalian neuronal differentiation. *EMBO J.* **18**, 2196-2207.

Ohtsuka, T., Sakamoto, M., Guillemot, F. and Kageyama, R. (2001). Roles of the basic helix-loop-helix genes Hes1 and Hes5 in expansion of neural stem cells of the developing brain. *J. Biol. Chem.* **276**, 30467-30474.

Ohtsuka, T., Shimojo, H., Matsunaga, M., Watanabe, N., Kometani, K., Minato, N. and Kageyama, R. (2011). Gene expression profiling of neural stem cells and identification of regulators of neural differentiation during cortical development. *Stem Cells* **29**, 1817-1828.

Okamoto, M., Miyata, T., Konno, D., Ueda, H. R., Kasukawa, T., Hashimoto, M., Matsuzaki, F. and Kawaguchi, A. (2016). Cell-cycle-independent transitions in temporal identity of mammalian neural progenitor cells. *Nat. Commun.* **7**, 11349.

Ozturk, N., Singh, I., Mehta, A., Braun, T. and Barreto, G. (2014). HMGA proteins as modulators of chromatin structure during transcriptional activation. *Front. Cell Dev. Biol.* **2**, 5.

Patterson, M., Gaeta, X., Loo, K., Edwards, M., Smale, S., Cinkornpumin, J., Xie, Y., Listgarten, J., Azghadi, S., Douglass, S. M. et al. (2014). let-7 miRNAs can act through notch to regulate human gliogenesis. *Stem Cell Rep.* **3**, 758-773.

Pereira, J. D., Sansom, S. N., Smith, J., Dobenecker, M.-W., Tarakhovsky, A. and Livesey, F. J. (2010). Ezh2, the histone methyltransferase of PRC2, regulates the balance between self-renewal and differentiation in the cerebral cortex. *Proc. Natl. Acad. Sci. USA* **107**, 15957-15962.

Robey, E., Chang, D., Itano, A., Cado, D., Alexander, H., Lans, D., Weinmaster, G. and Salmon, P. (1996). An activated form of Notch influences the choice between CD4 and CD8 T cell lineages. *Cell* **87**, 483-492.

Sakamoto, M., Hirata, H., Ohtsuka, T., Bessho, Y. and Kageyama, R. (2003). The basic helix-loop-helix genes Hesr1/Hey1 and Hesr2/Hey2 regulate maintenance of neural precursor cells in the brain. *J. Biol. Chem.* **278**, 44808-44815.

Salic, A. and Mitchison, T. J. (2008). A chemical method for fast and sensitive detection of DNA synthesis in vivo. *Proc. Natl. Acad. Sci. USA* **105**, 2415-2420.

Sanosaka, T., Namihira, M., Asano, H., Kohyama, J., Aisaki, K., Igarashi, K., Kanno, J. and Nakashima, K. (2008). Identification of genes that restrict astrocyte differentiation of midgestational neural precursor cells. *Neuroscience* **155**, 780-788.

Schwartz, Y. B. and Pirrotta, V. (2013). A new world of Polycombs: unexpected partnerships and emerging functions. *Nat. Rev. Genet.* **14**, 853-864.

Tan, S.-L., Nishi, M., Ohtsuka, T., Matsui, T., Takemoto, K., Kamio-Miura, A., Aburatani, H., Shinkai, Y. and Kageyama, R. (2012). Essential roles of the histone methyltransferase ESET in the epigenetic control of neural progenitor cells during development. *Development* **139**, 3806-3816.

Tanigaki, K., Nogaki, F., Takahashi, J., Tashiro, K., Kurooka, H. and Honjo, T. (2001). Notch1 and Notch3 instructively restrict bFGF-responsive multipotent neural progenitor cells to an astroglial fate. *Neuron* **29**, 45-55.

Temple, S. (2001). The development of neural stem cells. *Nature* **414**, 112-117.

Vogel, T., Stoykova, A. and Gruss, P. (2006). Differential expression of polycomb repression complex 1 (PRC1) members in the developing mouse brain reveals multiple complexes. *Dev. Dyn.* **235**, 2574-2585.

Weinmaster, G. (1997). The ins and outs of Notch signaling. *Mol. Cell. Neurosci.* **9**, 91-102.

Fig. S1

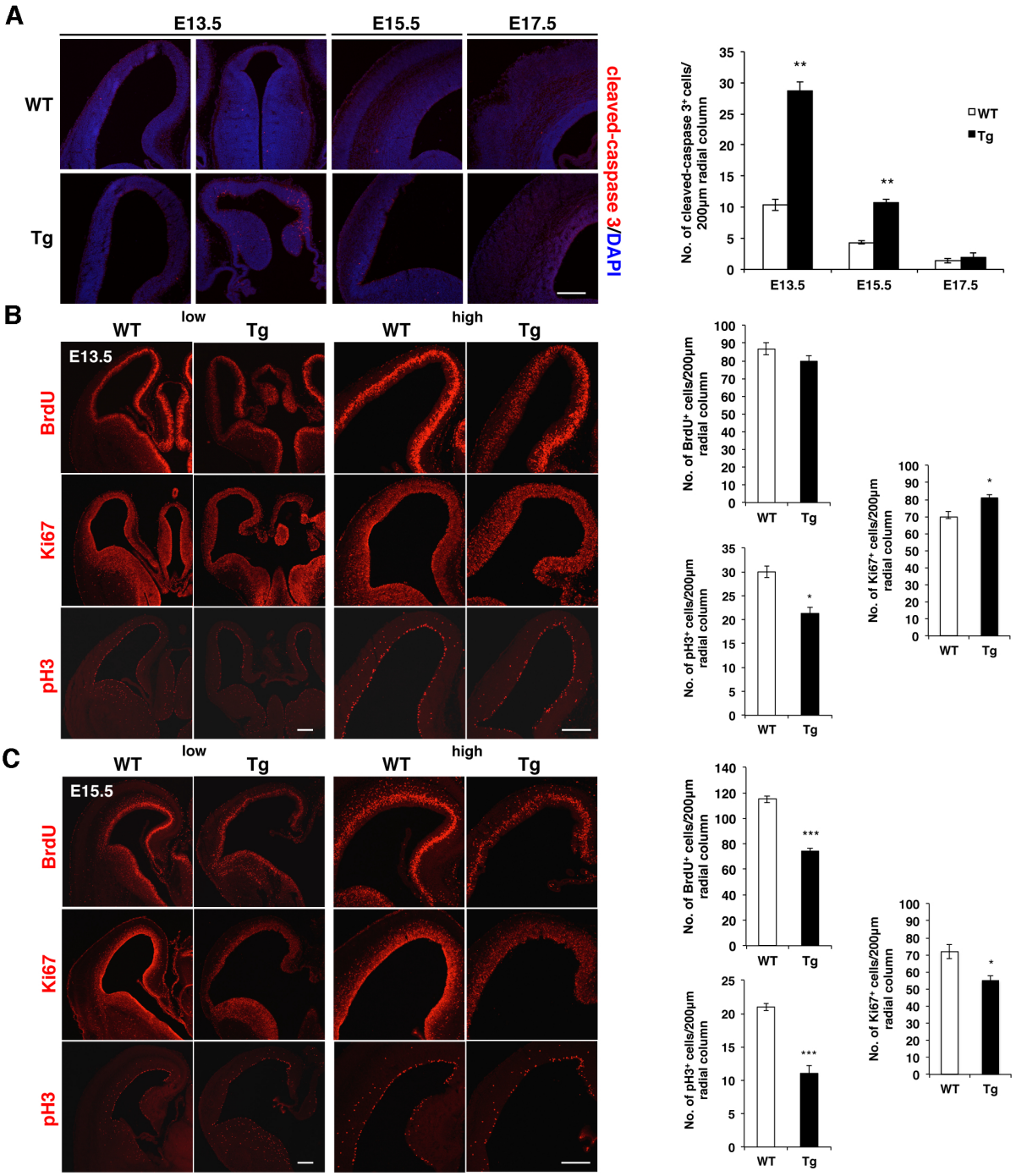

Fig. S1. Analyses of cell death and cell proliferation activity. (**A**) Estimation of cell death by immunohistochemistry using anti-cleaved-caspase 3 antibodies on coronal sections of the telencephalon of WT and Hes5-overexpressing Tg mice at E13.5, E15.5 and E17.5. DAPI (blue) for nuclear staining. Graphs showing the numbers of cleaved-caspase 3^+ cells in a radial column of 200 μm width in the neocortical regions. (**B**,**C**) Analyses of cell proliferation activity at E13.5 (B) and E15.5 (C). BrdU was administered intraperitoneally to pregnant mice 30 minutes before sacrifice. Immunohistochemistry was performed using antibodies against BrdU, Ki67 and pH3 (red) on coronal sections of neocortical regions of WT and Tg brains to estimate the number of cells that incorporated BrdU during S phase, $Ki67^+$ proliferating cells, and $pH3^+$ dividing cells at M phase. Magnified images are shown in the right panels. Graphs showing the numbers of $BrdU^+$, $Ki67^+$, and $pH3^+$ cells in a radial column of 200 μm width in the neocortical regions. n=3, error bars: s.e.m.; *P<0.05, **P<0.01, ***P<0.001; Student's t-test. Scale bars: 200 μm.

Fig. S2

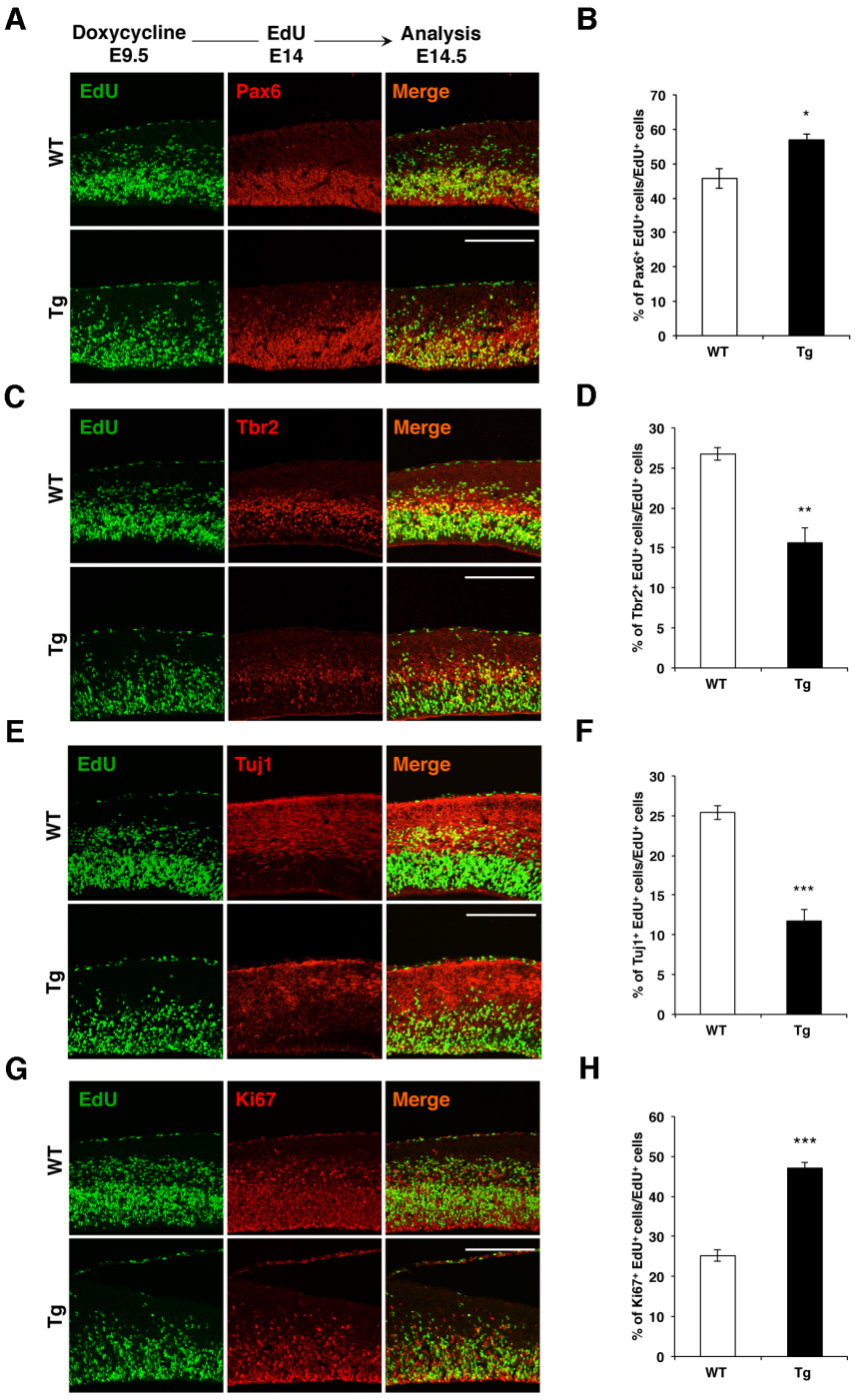

Fig. S2. Self-renewal versus cell cycle exit and differentiation of NSCs. (**A**,**C**,**E**,**G**) Analysis of self-renewal versus cell cycle exit of EdU-incorporated cells in the neocortical regions of WT and Hes5-overexpressing Tg brains. Dox was administered from E9.5 onward. EdU was administered intraperitoneally to pregnant mice at E14, and embryos were fixed 12 hours later at E14.5. The fates of EdU^+ cells were examined by immunostaining using Pax6 (A), Tbr2 (C), Tuj1 (E), and Ki67 (G) antibodies. (**B**,**D**,**F**,**H**) Graphs showing the proportions of cells positive for each marker among EdU^+ cells. Total numbers of EdU^+ cells counted for the quantification were at least 200 cells for each analysis. n=3, error bars: s.e.m.; *P<0.05, **P<0.01, ***P<0.001; Student's t-test. Scale bars: 200 µm.

Fig. S3

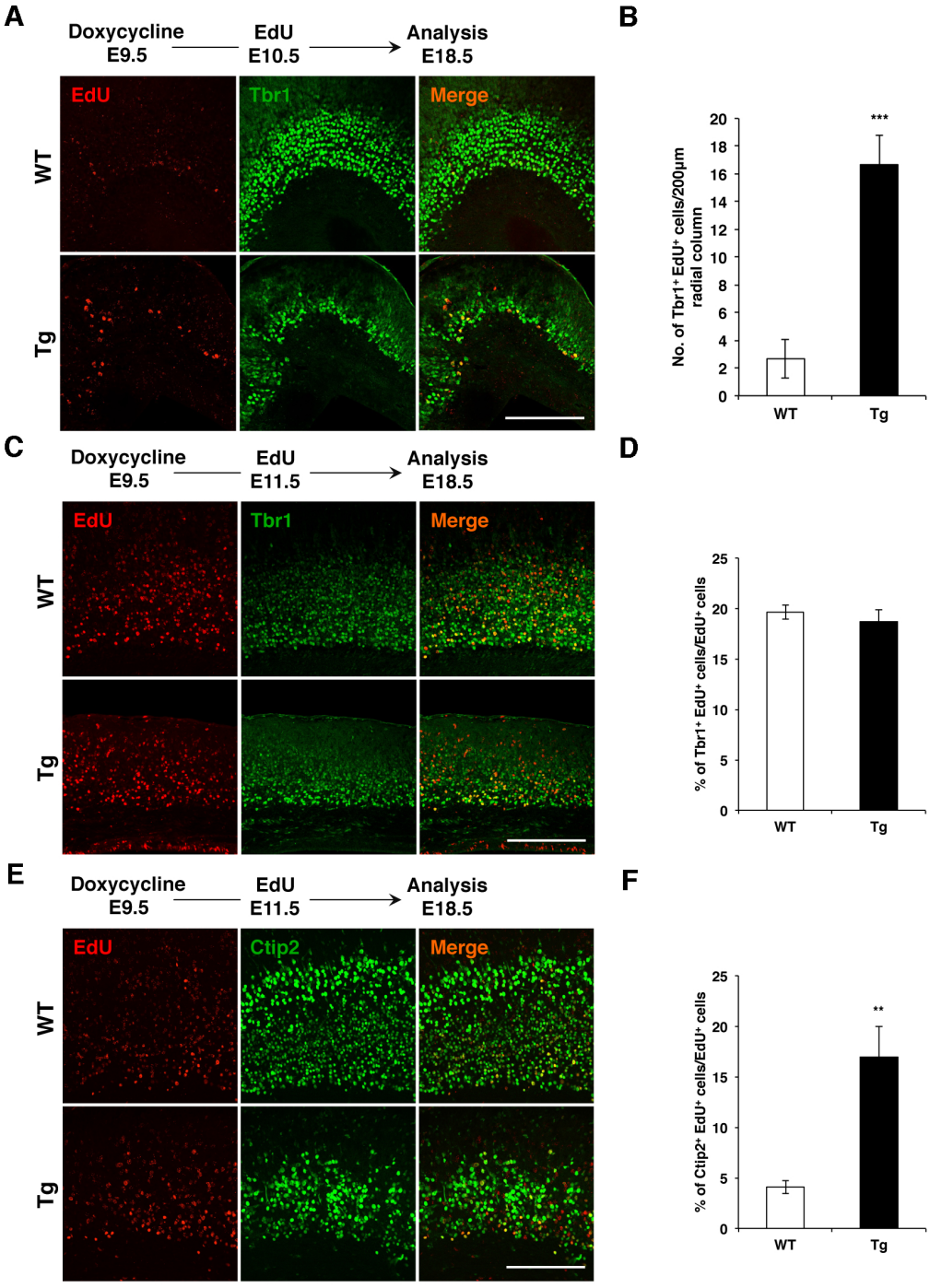

Fig. S3. Analyses of the early neurogenesis. (**A**,**C**,**E**) Birth date analysis of cortical neurons in the WT versus Hes5-overexpressing Tg brains. Dox was administered from E9.5 onward. EdU was administered at E10.5 (A) or E11.5 (C,E), and location and fates of EdU-incorporated cells (red) were examined by the layer-specific markers Tbr1 (A,C) and Ctip2 (E) (green) at E18.5. (**B**) Graph showing the numbers of cells co-labeled with EdU and Tbr1 in a radial column of 200 µm width in the neocortical regions. (**D**,**F**) Graphs showing the proportions of layer-specific neurons among EdU$^+$ cells. Total numbers of EdU$^+$ cells counted for the quantification were at least 100 cells for each analysis. n=3, error bars: s.e.m.; ***P<0.001; Student's t-*t*est. Scale bars: 200 µm.

Fig. S4

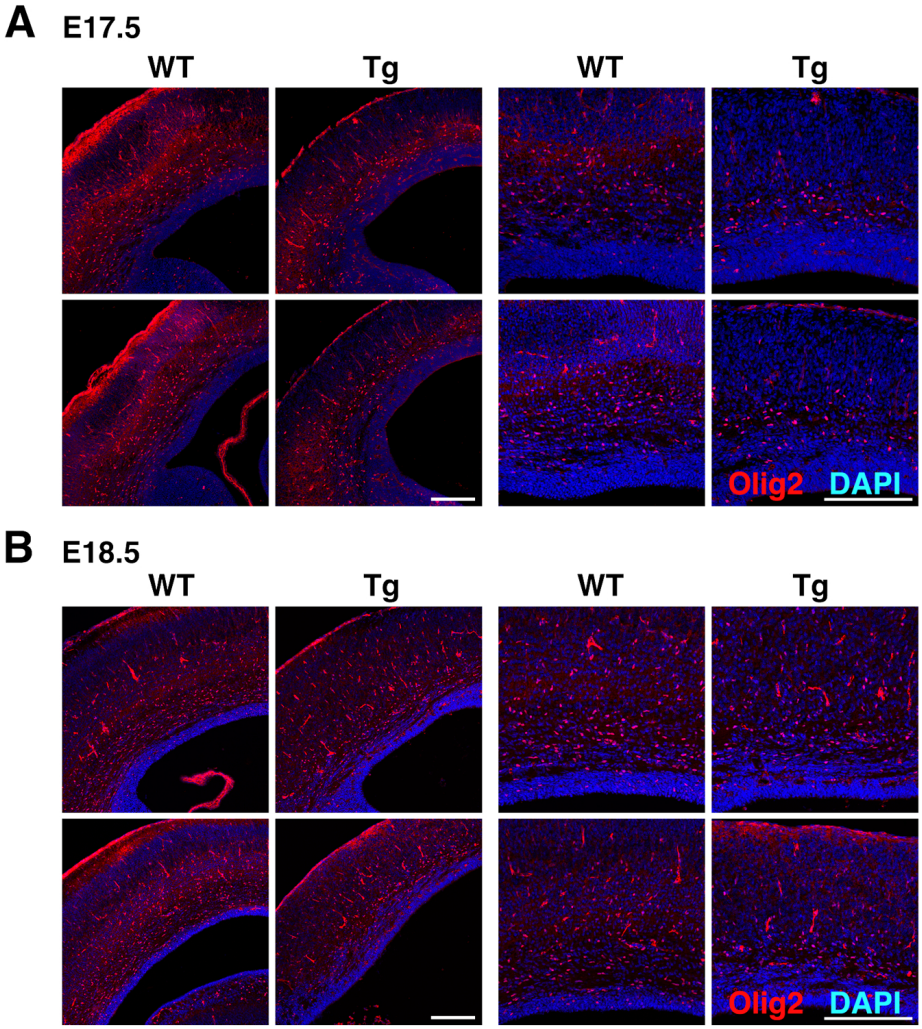

Fig. S4. Analysis of generation of oligodendrocyte lineage. Immunostaining was performed using anti-Olig2 antibodies (red) on coronal sections of the neocortical regions of WT and Hes5-overexpressing Tg brains at E17.5 (A) and E18.5 (B). Magnified images are shown in the right panels. DAPI (blue) for nuclear staining. Scale bars: 200 μm.

Fig. S5

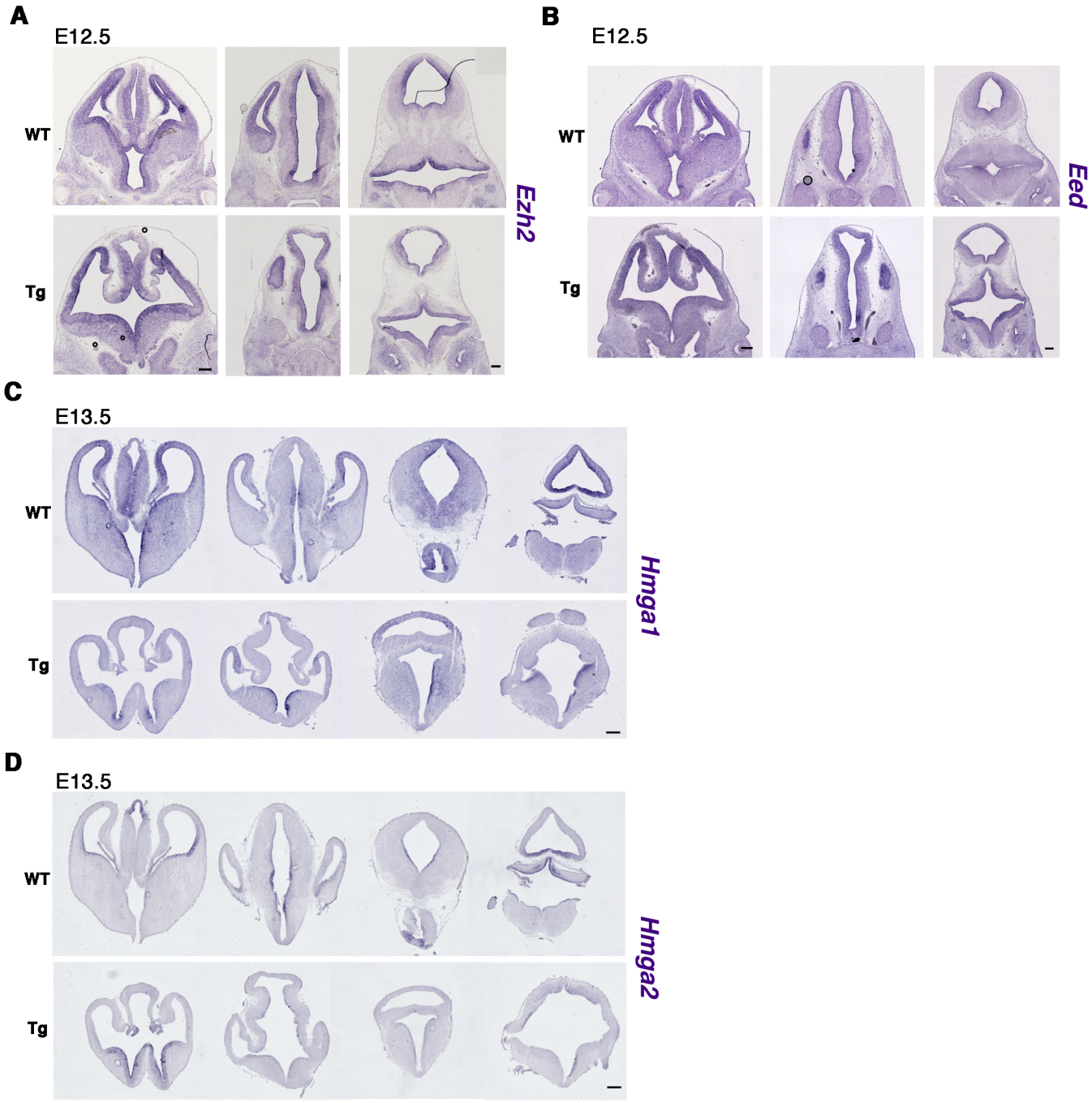

Fig. S5. Expression of *Ezh2*, *Eed*, and *Hmga* genes throughout the brain. (**A**,**B**) *In situ* hybridization for mRNA expression of *Ezh2* (A) and *Eed* (B) on coronal sections of forebrain (left) through hindbrain (right) of WT and Hes5-overexpressing Tg brains at E12.5. (**C**,**D**) *In situ* hybridization for mRNA expression of *Hmga1* (C) and *Hmga2* (D) on coronal sections of forebrain (left) through hindbrain (right) of WT and Hes5-overexpressing Tg brains at E13.5. Scale bars: 200 µm.

Table S1. Primary antibodies

Antigen	Host	Manufacturer	Catalogue No.	Dilution
GFP	chicken	Molecular Probes	A11122	1:500
Hes1	rabbit	Cell Signaling	#11988S	1:100
Pax6	rabbit	Covance	PRB-278P	1:200
Tbr2	rabbit	Abcam	ab23345	1:500
Tuj1	mouse	Covance	MMS-435P	1:1000
NeuN	mouse	Merck Millipore	MAB337	1:500
Tbr1	rabbit	Abcam	ab31940	1:400
Ctip2	rat	Abcam	ab18465	1:500
Cux1	rabbit	Santa Cruz	sc-13024	1:100
GFAP	rabbit	DAKO	Z0334	1:500
GFAP	rabbit	Sigma-Aldrich	G9269	1:400
BrdU	rat	Serotec	MCA2060	1:500
Ki67	mouse	BD Pharmingen	556003	1:100
pH3	mouse	Sigma-Aldrich	H6409	1:500
Olig2	mouse	EMD Millipore	MABN50	1:500
Cleaved caspase-3	rabbit	Cell Signaling	#9661S	1:500

Table S2. qRT-PCR primers

Gene	Primer	Sequence
Hes1	Fw (Forward)	5′-TGAAGGATTCCAAAAATAAAATTCTCTGGG-3′
	Rv (Reverse)	5′-CGCCTCTTCTCCATGATAGGCTTTGATGAC-3′
Hes5	Fw	5′-AAGTACCGTGGCGGTGGAGATGC-3′
	Rv	5′-CGCTGGAAGTGGTAAAGCAGCTT-3′
Neurog2	Fw	5'- TCGCCAGGGACTGTATCT-3'
	Rv	5'-CTGTGAAGTGGAGTCCG-3'
Ascl1	Fw	5′-GCCACCAGAATGACTTCAGCAC-3′
	Rv	5′-AAGGCAACCTATGGGAACCAAC-3′
Tbr1	Fw	5′-CCGAGTCCAGACGTTCACTT-3′
	Rv	5′-GCCCGTGTAGATCGTGTCAT-3′
Ctip2	Fw	5′-ACGACAAGGTCCTGGACAAG-3′
	Rv	5′-TTGTGCAAATGAGCTGGAAG-3′
Fezf2	Fw	5′-CTCTACTGACAGCAAACCCA-3′
	Rv	5′-CTTTGCACACAAACGGTCT-3′
Cux1	Fw	5′-CAGCGCTTATTTGGGGAGACC-3′
	Rv	5′-TGGAACCAGTTGATGACGGTG-3′
GFAP	Fw	5'-GGCGCTCAATGCTGGCTTCA-3′
	Rv	5′-TCTGCCTCCAGCCTCAGGTT-3′
Ezh2	Fw	5′-TTTGCTAATCATTCAGTAAATCCAAAC-3′
	Rv	5′-GCAAAGATGCCTATCCTGTG-3′
Eed	Fw	5'-GTATGTTTGGGATTTAGAAGTAGAAGA-3'
	Rv	5'-CTACTGAAACTGGTTTGTCGAA-3'
Ring1B	Fw	5′-AGTTACAACGAACACCTCAG-3′
	Rv	5′-TCCAAACAAATTGGGCACAT-3′
Hmga1	Fw	5'-CATCTCACTCTGACAAGGC-3′
	Rv	5'-CACCCGGTGATACTTTGG-3′
Hmga2	Fw	5'-AGAACTAGACACTACTCTCCTT-3′
	Rv	5'-CGAGCATAACCTATTCTGGTTT-3′
Gapdh	Fw	5′-TGGGTGTGAACCACGA-3′
	Rv	5′-AAGTTGTCATGGATGACCTT-3′